Design and Implementation of an Educational High-Power Inductive Wireless Power Transfer Setup

Stijn Verhaeghe
Faculty of Engineering Technology
KU Leuven
Ghent, Belgium
stijn.verhaeghe@student.kuleuven.be

Arthur Cloet
Department of ESAT
KU Leuven
Ghent, Belgium
arthur.cloet@kuleuven.be

Michael Kleemann
Department of ESAT
KU Leuven
Ghent, Belgium
michael.kleemann@kuleuven.be

Jarne Van Mulders
DRAMCO
KU Leuven
Ghent, Belgium
jarne.vanmulders@kuleuven.be

***Abstract*—This paper presents the design and implementation of a 500 W educational Inductive Wireless Power Transfer (IWPT) setup, developed to address the current lack of accessible high-power educational platforms. The system utilizes an LCC-S compensation topology, specifically selected for its ability to maintain a constant transmitting coil current and operate as a quasi-constant voltage source at a nominal frequency of 85 kHz. The hardware implementation consists of a transmitting unit that includes a full-bridge inverter, a dedicated controller, and the LCC compensation network. The receiving unit features series (S) compensation and a bridge rectifier. Experimental results demonstrate a peak efficiency of approximately 78% at an output power of 393 W. Furthermore, an integrated laboratory curriculum was developed to focus on functional block identification, simulation-to-practical verification, and the impact of coil misalignment in robotic applications. This setup effectively bridges the gap between theoretical knowledge and practical high-power IWPT challenges, providing students with critical insights into industrial power transfer systems.**

***Index Terms*—Inductive Wireless Power Transfer (IWPT), LCC-S compensation, High-power and Educational setup**

I. Introduction

INDUCTIVE Wireless Power Transfer (IWPT) is increasingly used in industrial robotics and electric vehicle charging. While the demand for expertise in this field grows, engineering education remains limited by existing hardware. Most educational WPT kits are restricted to low power levels (under 50 W) [1], which prevents students from exploring the challenges and dynamics of high-power energy transmission.

To bridge this gap, this paper presents a 500 W educational IWPT setup. The system operates at a nominal frequency of 85 kHz and utilizes an LCC-S compensation topology. This specific topology was chosen because it ensures a constant current in the transmitting coil and acts as a quasi-constant voltage source.

The primary contribution of this work is the development of a high-power hardware platform integrated with a laboratory assignment. This allows students to study the different IWPT-blocks and the impact of coil misalignment through both simulation and practical measurements.

The remainder of this paper is structured as follows: Section II provides the theoretical analysis of the LCC-S topology. Section III describes the hardware implementation. Section IV presents the experimental results obtained with the setup. Section V discusses the motivation and development of the educational laboratory assignment. Finally, Section VI concludes the paper and offers suggestions for future work.

II. System Architecture and Theoretical Analysis

A. General System Configuration

The architecture of the developed IWPT system is composed of five primary functional stages, as illustrated in the block diagram in fig. 1 [2]. At the transmitting side, an inverter converts the voltage from a DC power source into a high-frequency alternating voltage. Subsequently, a compensation (resonant) network is employed to ensure operational stability and enhance system efficiency.

The energy transfer itself can be realized in two ways: via inductive or capacitive coupling. In this specific setup, the inductive method is utilized. On the receiving side, the system likewise contains a compensation network, followed by a bridge rectifier that converts the received AC voltage back into a stable DC output to power the load.

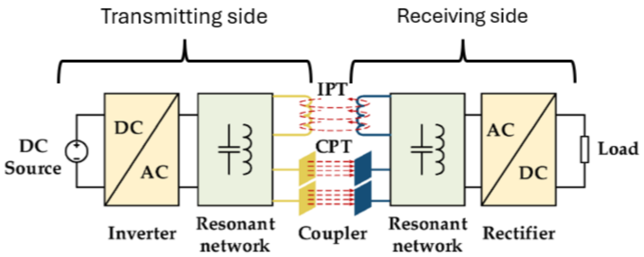

Fig. 1. General block diagram of a Wireless Power Transfer (WPT) system [2].

B. LCC-S Compensation Topology

Energy transfer can be achieved using fundamental topologies such as Series-Series (SS), Series-Parallel (SP), Parallel-Series (PS), and Parallel-Parallel (PP). However, these networks often face limitations regarding load independence and efficiency under varying coupling conditions [3]. To overcome these challenges, this setup utilizes an advanced higher-order Inductor-Capacitor-Capacitor-Series (LCC-S) topology.

The LCC-S configuration consists of a compensation inductor and two capacitors on the transmitting side, paired with a single series compensation capacitor on the receiving side. The primary advantages of this network include:

- **Constant Coil Current:** The primary LCC network ensures that the current in the transmitting coil remains constant, regardless of load variations.
- **Load-Independent Voltage:** The system behaves as a quasi-constant voltage source, providing stability for the output stage.

As illustrated in fig. 2, the topology can be analyzed through three distinct functional blocks [3]:

- **Block 1:** At resonance, this stage ensures the system acts as a constant current source.
- **Block 2:** Forms the main resonant circuit for energy transfer on the primary side.
- **Block 3:** Acts as a constant voltage source on the secondary side.

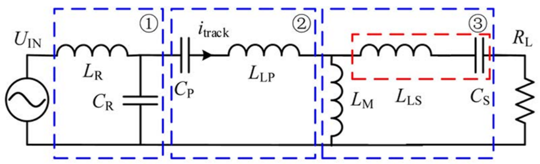

Fig. 2. Simplified circuit diagram of the LCC-S compensation topology divided into functional blocks [3].

To achieve these load-independent characteristics, the components must be precisely tuned to the angular resonance frequency ω_0. Following the circuit parameters shown in fig. 3, the resonance conditions are defined as [4]:

First, the primary resonance is established by L_1 and C_1:

$$\omega_0 L_1 = \frac{1}{\omega_0 C_1} \implies C_1 = \frac{1}{\omega_0^2 L_1} \tag{1}$$

The primary series capacitor C_2 is determined by the difference between the primary coil inductance L_2 and the compensation inductor L_1:

$$\omega_0 (L_2 - L_1) = \frac{1}{\omega_0 C_2} \implies C_2 = \frac{1}{\omega_0^2 (L_2 - L_1)} \tag{2}$$

Finally, the secondary side is tuned by matching C_3 with the secondary coil L_3:

$$\omega_0 L_3 = \frac{1}{\omega_0 C_3} \implies C_3 = \frac{1}{\omega_0^2 L_3} \tag{3}$$

Under these conditions, the current in the transmitting coil (I_{track}) becomes independent of the load:

$$I_{track} = \frac{U_{IN}}{j\omega_0 L_1} \tag{4}$$

Based on this mathematical framework, the component values for the 500 W prototype were calculated for an operating frequency of 85 kHz. These implemented values are summarized in table I, and the corresponding detailed circuit schematic is provided in fig. 3.

TABLE I
SYSTEM DESIGN PARAMETERS AND COMPONENT VALUES

Parameter	Symbol	Value
Operating Frequency	f_0	85 kHz
Primary Compensation Inductor	L_1	4.7 μH
Primary Parallel Capacitor	C_1	750 nF
Primary Series Capacitor	C_2	2.7 μF
Secondary Series Capacitor	C_3	580 nF
Primary Coil Inductance	L_2	5.8 μH
Secondary Coil Inductance	L_3	5.8 μH

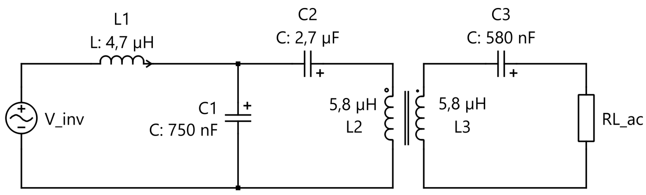

Fig. 3. Detailed circuit schematic of the implemented LCC-S network with specific component values for 85 kHz resonance.

III. HARDWARE IMPLEMENTATION

The hardware design of the educational IWPT system is engineered to handle a maximum power of 500 W at an operating frequency of 85 kHz. The system is split into two primary units: the transmitting (primary) unit and the receiving (secondary) unit.

A. Transmitting Unit

The transmitting unit is responsible for converting the DC input into a high-frequency AC magnetic field. This unit integrates the power electronics stage, control logic, and the primary compensation network into a single high-power assembly, as displayed in fig. 4.

1) Full-Bridge Inverter and Thermal Management: The core of the transmitting unit is a high-frequency full-bridge inverter. To implement this, two Infineon EVAL_2EDB_HB_GAN half-bridge evaluation boards are utilized in a coordinated configuration [5]. This setup leverages CoolGaN™ technology, which allows for efficient switching at the target frequency of 85 kHz.

To ensure reliable operation, the unit is equipped with active cooling:

- **Intake Fan:** Positioned to blow fresh air directly through the heatsink fins of the inverter modules.

- **Exhaust Fan:** Responsible for removing warm air from the enclosure to maintain a stable internal temperature.

2) Control and User Interface: The inverter is controlled by an **ESP32-Wrover** microcontroller, which generates the high-frequency Pulse Width Modulation (PWM) signals required for the gate drivers. To enhance the educational utility of the setup, the system features a manual frequency adjustment mechanism:

- **Frequency Control:** A potentiometer is interfaced with the ESP32, allowing users to sweep the operating frequency around the nominal 85 kHz resonance point.
- **Visual Feedback:** An integrated LCD display provides real-time feedback of the current operating frequency.
- **Signal Generation:** The ESP32 maintains precise timing and dead-time insertion, preventing cross-conduction in the GaN half-bridges.

3) Primary LCC Network and Connectivity: Immediately following the inverter, the primary LCC network is integrated on a dedicated PCB. To ensure the robustness of the compensation stage:

- **Parallel Capacitor Design:** Similar to the receiving unit, the capacitors in the LCC network (C_1 and C_2, as shown in fig. 3) consist of multiple parallel-connected film capacitors. This configuration is critical for handling the high reactive power and circulating currents typical for LCC topologies, effectively distributing the current to minimize self-heating.
- **Diagnostic Test Points:** The PCB is equipped with accessible test points, enabling students to measure the voltage waveforms across the compensation inductor (L_1), the capacitor banks, and the output to the transmitting coil.

The connection to the transmitting coil is established via a high-current **XT60 connector**, ensuring low contact resistance and ease of use in a laboratory environment.

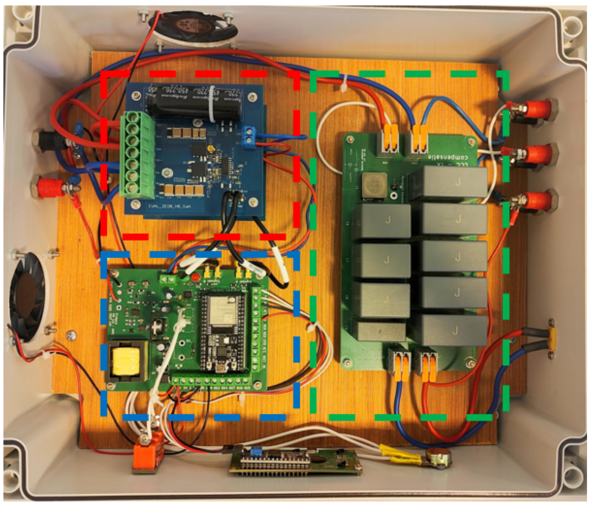

Fig. 4. The implemented transmitting unit with annotated sections: the ESP32 control stage (blue), the Infineon GaN full-bridge inverter (red), and the primary LCC compensation network with parallel capacitor banks (green).

B. Inductive Link and Coil Design

The inductive link is the critical interface for IWPT-system. As shown in fig. 5, the link consists of two identical planar spiral coils.

To ensure high efficiency at the 85 kHz operating frequency, several design choices were made:

- **Litz Wire:** The windings are constructed using Litz wire to mitigate the skin effect and proximity effect, which significantly increase AC resistance at high frequencies.
- **Ferrite Shielding:** Each coil is backed by a ferrite plate. This serves to guide the magnetic flux and shield the surrounding electronics from electromagnetic interference (EMI).
- **Mechanical Alignment:** For experimental consistency, a custom wooden fixture is used to maintain a fixed distance and alignment between the primary and secondary coils, representing a nominal coupling factor k.

The physical parameters of the coils, such as the number of turns and diameter, are designed to match the inductance values L_2 and L_3 (nominally 5.8 μH) used in the theoretical resonance calculations in Section II.

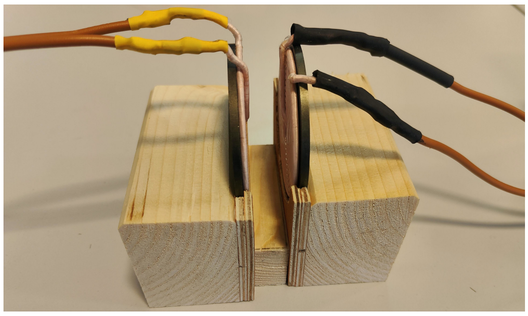

Fig. 5. Experimental setup of the inductive link showing the two planar coils with ferrite backing, mounted in an alignment fixture.

C. Receiving Unit

The receiving unit is responsible for capturing the high-frequency magnetic field and converting it into a stable DC output. This unit, housed in a dedicated enclosure, integrates the secondary compensation network and the power rectification stage, as illustrated in fig. 6.

1) Secondary Compensation and Rectification: Following the LCC-S topology requirements, the receiving side utilizes a series compensation scheme. The hardware implementation on the secondary PCB consists of several key stages:

- **Parallel Resonant Capacitor Bank (C_3):** To match the secondary coil inductance L_3, a bank of high-voltage film capacitors is employed. These capacitors are connected in a parallel configuration to increase the current-handling capacity of the network. This distribution of the RMS current across multiple components reduces thermal stress and prevents dielectric breakdown during 500 W operation.
- **Passive Full-Bridge Rectifier:** The 85 kHz AC induced in the secondary coil is converted to DC using a bridge

rectifier. This bridge consists of four fast-recovery diodes (D_1 through D_4), optimized for high-frequency switching.

- **Thermal Management:** Given the 500 W power rating, each diode is equipped with an individual black anodized aluminum heatsink. This passive cooling setup ensures that the thermal stress remains within safe limits during prolonged operation.

2) Connectivity and Educational Features: The unit is designed with educational transparency in mind. The PCB features a clear silk-screen diagram of the "S-RX compensation + passieve gelijkrichter," providing students with a direct link between the theoretical circuit and the physical layout.

For connectivity and advanced diagnostics, the following are integrated:

- **Comprehensive Measurement Points:** Dedicated test points are provided on the PCB to allow students to measure the voltage waveforms across both the compensation network and the receiving coil (L_3).
- **High-Current Terminals:** WAGO-style lever connectors are used for the input from the secondary coil and the DC output, ensuring low contact resistance and easy reconfiguration.

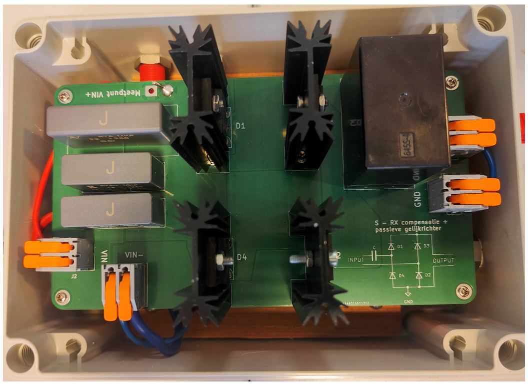

Fig. 6. Internal hardware of the receiving unit: the parallel C_3 capacitor bank (left), the four-diode rectifier bridge with dedicated heatsinks (center), output capacitor (right).

IV. Experimental Results and Discussion

To validate the performance of the developed IWPT system, a series of measurements were conducted focusing on output power characteristics, load regulation, and overall system efficiency. The system was tested at a nominal frequency of 85 kHz.

A. Power Transfer and Coupling Analysis

The relationship between the coupling coefficient (k) and the output power (P_{out}) for various input voltages is illustrated in fig. 7. As expected, the output power increases significantly with both the input voltage and the coupling factor. At the maximum tested input voltage of 60V and a high coupling coefficient of 0.8, the system achieves an output power approaching 400 W.

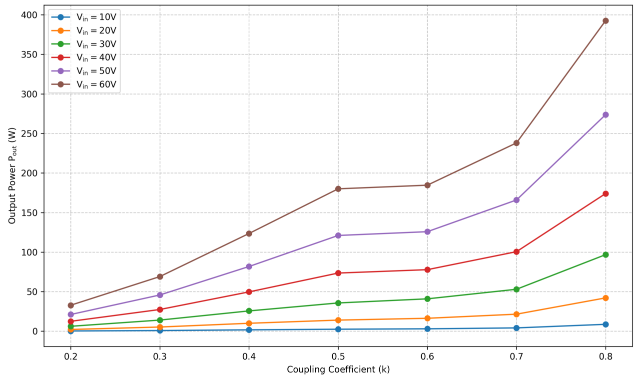

Fig. 7. Output power versus coupling coefficient (k) for various input voltages (V_{in} = 10V to 60V).

B. Load Independence Verification

A key theoretical advantage of the LCC-S topology is its ability to act as a quasi-constant voltage source. To verify this, the load resistance was varied from 5 Ω to 21 Ω while maintaining a constant input voltage. fig. 8 shows the measured output voltage (V_{out}).

The results show a remarkably stable output voltage, fluctuating only slightly between 34V and 40V over a wide load range. This confirms the load-independent voltage characteristics mentioned in Section II, which are essential for stable power delivery without complex active control loops.

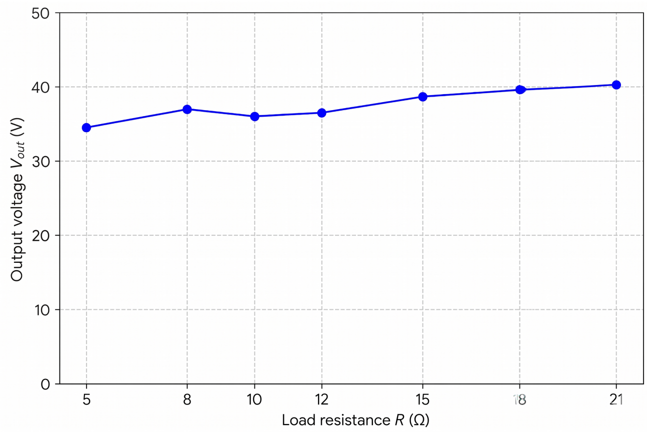

Fig. 8. Measured output voltage (V_{out}) across a variable load resistance (5–21 Ω), demonstrating the quasi-constant voltage characteristic.

C. Efficiency Performance

The system efficiency (η) was measured with a constant load of 5 Ω across various power levels. As illustrated in fig. 9, the efficiency shows a steep increase at lower power levels before stabilizing as the throughput power rises.

Key observations from the measurements include:

- **Peak Performance:** The system reaches a maximum efficiency of 78.87% at an output power of 392.8 W, corresponding to an input voltage of 60V.
- **Power Scaling:** Even at a moderate input of 20V, the efficiency already surpasses 76.6%, maintaining a very

stable plateau between 76% and 79% for the remainder of the power range.

- **Loss Analysis:** The relatively lower efficiency at the 10 V input level (63.31%) is primarily attributed to the conduction and switching losses within the full-bridge inverter and the passive bridge rectifier. At these lower power levels, the fixed forward voltage drop of the rectifier diodes and the relative overhead of the inverter's switching transitions represent a significant fraction of the total power. It should be noted that these measurements represent the power stage efficiency, excluding the auxiliary power consumption of the cooling fans and the ESP32 microcontroller. As the input voltage and total transmitted power increase, the impact of these semiconductor-related losses diminishes relative to the total energy transfer, leading to improved overall performance.

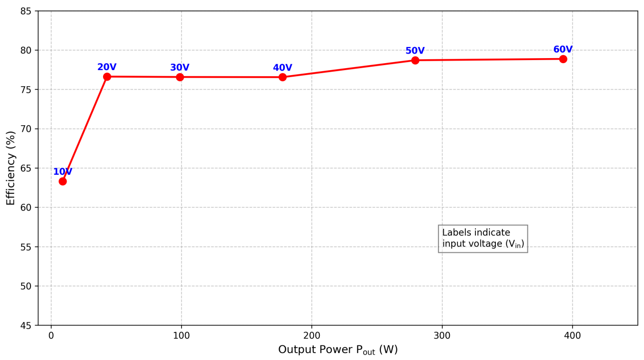

Fig. 9. System efficiency versus output power for a 5 Ω load with a coupling of 0,8. The blue labels indicate the corresponding input voltages (V_{in}) for each data point.

V. Educational Implementation and Laboratory Curriculum

The primary objective of the developed hardware is its integration into the "Sensors and Actuators" course at KU Leuven. To bridge the gap between theoretical power electronics and practical high-power applications, a comprehensive laboratory assignment was developed. The curriculum is structured around four key learning objectives (D1–D4).

A. System Architecture Analysis (D1)

The first phase of the curriculum focuses on decomposing the IWPT architecture into its fundamental building blocks. Students identify the roles of the inverter, the inductive link, and the rectification stage. A significant emphasis is placed on the **LCC-S compensation network**. Through preparatory assignments, students must justify the selection of this topology and use design equations to verify that the system operates as a quasi-constant voltage source.

B. Simulation-Based Verification (D2)

Before engaging with the physical hardware, students utilize a PLECS simulation model to predict system behavior. To focus on the IWPT-specific dynamics, the model simplifies the power stages by representing the inverter as an AC source and the rectified load as an equivalent AC resistance.

- **Frequency Domain:** Students simulate the frequency response to observe voltage and current gains under varying loads.
- **Time Domain:** Waveform analysis of individual components is performed to understand switching stresses.

C. Experimental Measurements and Misalignment (D3)

The practical component of the lab focuses on real-world constraints. A key experiment involves **misalignment in robotic applications**, mimicking an autonomous mobile robot docking over a floor-integrated charging pad.

The experimental setup used for these measurements is shown in fig. 10. Students perform a step-wise increase of the lateral misalignment between the primary and secondary coils to determine the operational limits of the setup. The objective is to quantify the coupling decay and identify the maximum displacement at which the output voltage remains above a functional threshold of 12 V. Finally, the experimental data are compared with simulation results to validate the quasi-constant voltage source characteristics of the LCC-S topology.

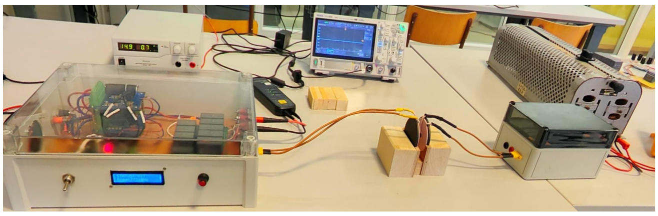

Fig. 10. 500 W educational IWPT setup used for misalignment measurements.

D. Comparative Analysis with Industrial Systems (D4)

To conclude the curriculum, students perform a high-level analysis of a commercial system, specifically the **Würth Elektronik 200 W Wireless Power Kit** [6]. While the educational setup operates in an open-loop configuration for simplicity, the industrial kit incorporates a closed-loop feedback mechanism.

Students study how the receiver communicates with the transmitter to maintain a stable output voltage despite coupling variations. This comparison highlights the transition from fundamental resonant power transfer to regulated commercial power solutions.

VI. Conclusion

This paper presented the design and implementation of a 500 W educational Inductive Wireless Power Transfer (IWPT) setup. By utilizing an LCC-S compensation topology, the system successfully demonstrates the characteristics of a quasi-constant voltage source at a nominal operating frequency of 85 kHz. Experimental results verified the robustness of the hardware, achieving a peak efficiency of approximately 78% at an output power of 393 W.

The integration of the hardware within a structured laboratory curriculum bridges the gap between theoretical power electronics and industrial practice. Through a combination of PLECS simulations and practical measurements, students gain critical insight into the trade-offs between coupling, efficiency, and stability. This analysis specifically focuses on coil misalignment within robotic docking scenarios. By linking these simulations to experimental data, the curriculum successfully demonstrates the real-world constraints of high-power wireless energy transfer. Furthermore, comparing this open-loop setup with industrial closed-loop systems provides a clear pathway for understanding advanced regulation and communication techniques.

Future work will involve the implementation of an active feedback loop to further enhance the educational scope, allowing students to study dynamic control strategies for maintaining stable power delivery under varying load and coupling conditions.

REFERENCES

[1] A. Bergmann, E. Dürr, and C. Rockstuhl, "Wireless power transfer experiments for a high-school physics lab," *Physics Education*, vol. 54, no. 5, p. 055 016, Jul. 2019. DOI: 10.1088/1361-6552/ab2c2c. [Online]. Available: https://doi.org/10.1088/1361-6552/ab2c2c.

[2] Y. Liu, L. Pan, S. Yao, J. Zhang, S. Cui, and C. Zhu, "A review on the recent development of high-frequency inverters for wireless power transfer," *Energies*, vol. 17, no. 20, 2024, ISSN: 1996-1073. DOI: 10.3390/en17205153. [Online]. Available: https://www.mdpi.com/1996-1073/17/20/5153.

[3] W. Zhang and C. C. Mi, "Compensation topologies of high-power wireless power transfer systems," *IEEE Transactions on Vehicular Technology*, vol. 65, no. 6, pp. 4768–4778, 2016. DOI: 10.1109/TVT.2015.2454292.

[4] H. Shen, X. Wang, L. Wang, and P. Sun, "Parameter design method based on lcc-s ipt system considering equivalent load model of rectifier," in *2023 6th International Conference on Energy, Electrical and Power Engineering (CEEPE)*, 2023, pp. 930–936. DOI: 10.1109/CEEPE58418.2023.10166892.

[5] Infineon Technologies AG, *Eval_2edb_hb_gan: Half-bridge board designed with coolgan™ git hemts and eicedriver™ 2edb8259y*, Application Note, Infineon Technologies AG, Munich, Germany, 2022. [Online]. Available: https://www.infineon.com/dgdl/Infineon-EVAL-2EDB-HB-GAN-Half-bridge-board-designed-with-CoolGaN-GIT-HEMTs-and-EiceDRIVER-2EDB8259Y-ApplicationNotes-v01_00-EN.pdf?fileId=8ac78c8c8412f8d3018450d16dcf4eb8.

[6] Würth Elektronik, *200 W wireless power transfer development kit*, Onderdeelnummer: 760308EMP, Würth Elektronik eiSos GmbH & Co. KG, Waldenburg, Germany, 2023. Accessed: May 22, 2024. [Online]. Available: https://www.we-online.com/en/support/kits-boards/200-w-wireless-power-kit.